

## Pore-pressure cycling experiments on Mx80 Bentonite

C. C. GRAHAM<sup>1\*</sup>, J. F. HARRINGTON<sup>1</sup>, R. J. CUSS<sup>1</sup> & P. SELLIN<sup>2</sup>

<sup>1</sup>*British Geological Survey, Keyworth, Nottingham NG12 5GG, UK*

<sup>2</sup>*Svensk Kärnbränslehantering AB, Stockholm, Sweden*

*\*Corresponding author (e-mail: caro5@bgs.ac.uk)*

**Abstract:** The Swedish concept for geological disposal of radioactive waste involves the use of bentonite as part of an engineered barrier system. A primary function of the bentonite is its ability to swell when hydrated by its surroundings. One particular uncertainty is the impact on this function, resulting from deviations in pore-water pressure,  $p_w$ , from expected *in situ* hydrostatic conditions. We present results from a series of laboratory experiments designed to investigate the form of the relationship between swelling pressure and  $p_w$ , for compacted Mx80 bentonite, from low to elevated applied water pressure conditions. The experiments were conducted using constant volume cells, designed to allow the total stresses acting on the surrounding vessel to be monitored (at five locations) during clay swelling. The results demonstrate that swelling pressure reduces non-linearly with increasing  $p_w$ , becoming less sensitive to changes at elevated pressures. After cyclic loading a marked hysteresis was also observed, with swelling pressure remaining elevated after a subsequent reduction in applied water pressure. Such behaviour may impact the mechanical and transport properties of the bentonite and its resulting performance. However, such hysteric behaviour was not always observed. Further testing is required to better understand the causes of this phenomenon and the controls on such behaviour.



**Gold Open Access:** This article is published under the terms of the CC-BY 3.0 license.

In the Swedish concept for disposal of radioactive waste, copper canisters containing the vitrified waste material are emplaced within a crystalline host-rock. The canisters are isolated from the surrounding rock by blocks and pellets of pre-compacted bentonite. The bentonite provides a number of functions within the design, including: (a) structural support, preventing collapse and protecting the canister from excessive stresses; (b) a diffusional barrier surrounding the canister; and (c) a swelling characteristic on hydration, which aids in the closure of voids and joints within the deposition hole. As such, the swelling properties of the bentonite are of primary importance to the design of the system. In order for the material to act as a successful barrier, it must be able to generate and maintain its expected swelling pressure,  $\Pi$  (when constrained by its surroundings), over long timescales.

Early experimental studies in bentonite demonstrated that the development of swelling pressure occurs rapidly in the initial stages of swelling, before notably reducing in rate as the final pressure is approached (Pusch 1980; Börgesson 1985; Madsen & Müller-Vonmoos 1989; Bucher & Müller-Vonmoos 1989). The rate of this development may be affected by factors such as the initial water content of the material and the applied water pressure. However, the final pressure achieved by the swelling bentonite, for a given pore water chemistry, is strongly dependent upon the initial dry density (Pusch 1980; Bucher &

Müller-Vonmoos 1989; Oscarson *et al.* 1990). A number of test geometries are commonly used for testing the swelling properties of clays; for example, a sample is allowed to swell under a specific load, or sample loading is achieved by constraining the sample from swelling. This latter approach, where sample volume is maintained constant, is the most representative of compacted bentonite blocks swelling in an enclosed engineered barrier system (EBS). As such, a constant volume arrangement was utilized in this study, in order to provide the most appropriate boundary condition.

The SKB safety case for a Swedish radioactive waste repository highlights the potential importance of long-term fluctuations in local pore-water pressures on repository functions (SKB 2011). For example, during future glaciation events, pore-water pressures are likely to be significantly elevated for considerable periods of time. One particular uncertainty is the likely effect of elevated pore-water pressures on the safety functions of the engineered barrier. Over the repository lifetime such changes in pore-water pressure may well be cyclic in nature, as successive glacial episodes lead to loading and unloading of the engineered barrier. It is therefore crucial to have a full understanding of the impact of such changes in pore-water pressure on the swelling properties of the bentonite. There are a considerable number of studies focussing on the impact of cyclic drying and wetting of clays and argillaceous rocks within the

*From:* NORRIS, S., BRUNO, J., CATHELIN, M., DELAGE, P., FAIRHURST, C., GAUCHER, E. C., HÖHN, E. H., KALINICHEV, A., LALIEUX, P. & SELLIN, P. (eds) 2014. *Clays in Natural and Engineered Barriers for Radioactive Waste Confinement*. Geological Society, London, Special Publications, **400**, 303–312.

First published online May 7, 2014, <http://dx.doi.org/10.1144/SP400.32>

© The Authors 2014. Publishing disclaimer: [www.geolosc.org.uk/pub\\_ethics](http://www.geolosc.org.uk/pub_ethics)

literature (Osipov *et al.* 1987; Basma *et al.* 1996; Pejón & Zuquette 2002; Doostmohammadi *et al.* 2008). However, there is a paucity of data relating to the impact of water pressure cycling on fully saturated clays at applied pressures in the vicinity of expected *in situ* conditions for a radioactive waste repository. The focus of this paper is on the effects of such deviations from hydrostatic conditions on bentonite, within the context of the Swedish radioactive waste disposal programme.

Bucher & Müller-Vonmoos (1989) investigated the development of stress generated by swelling of Mx80 and Montigel bentonite. They observed a strong correlation between swelling stress,  $\sigma$ , and increased dry density. By applying stepped increases in the applied water pressure, the consequent increase in  $\sigma$  was determined in order to delineate the relationship between the two. For samples of dry density below  $1.40 \text{ mg mm}^{-3}$ , this relationship was seen to be approximately linear, although the full range of potential water pressures expected in the repository environment was not examined; instead, low to moderate pressures were considered only. However, for higher dry densities, swelling stress was observed to be less sensitive to increasing  $p_w$ , with a generated value of only 60–70% of the applied water pressure, for a dry density of  $1.90 \text{ mg m}^{-3}$ . The authors suggested that this observed deviation from the standard effective stress law (Terzaghi 1943) may be at least partly explained by the exceptionally small pore volume in highly compacted bentonite, which clearly limits the availability of free water within the material. While Terzaghi's principal requires that the effective stress, or 'swelling pressure' for clays, results from the difference between generated stress and the applied pore pressure, Bucher and Müller-Vonmoos suggested the addition of a proportionality constant to allow for this deviation from linear behaviour.

Harrington & Horseman (2003) and Harrington & Birchall (2007) also observed this deviation for Mx80 bentonite, under a constant volume boundary condition. When investigating the change in total stress,  $d\sigma$ , resulting from a change in applied water pressure,  $dp_w$ , their observations also required the introduction of a proportionality constant,  $\alpha$  (equal to  $d\sigma/dp_w$ ), to adequately describe them. As such, for a clay–water system with the pore-water in thermodynamic equilibrium with an external reservoir of water at pressure,  $p_w$ , the total stress acting on the surrounding vessel can be expressed as:

$$\sigma = \Pi + \alpha p_w \quad (1)$$

where  $\Pi$  is the swelling pressure. This is the definition for swelling pressure used in this study and throughout the remainder of this paper.

While it has been previously suggested that, with increasing applied water pressure, the swelling pressure may decline to the point where liquefaction of the bentonite occurs, the findings from a number of studies contradict this (Harrington & Horseman 2003), instead indicating that, for higher-density bentonite, swelling pressure becomes increasingly insensitive to changes in applied water pressure at elevated values of  $p_w$ . The same observation is made in this paper, where the form of this relationship is examined at higher applied water pressures.

We present observations from constant volume experiments on four bentonite samples (Mx80-10, -11, -13 and -14), focussed on elucidating the relationship between  $p_w$  and  $\Pi$ . The samples tested were prepared from blocks of pre-compacted Mx80 bentonite, which is a candidate clay for the Swedish repository concept. The data from testing specimens Mx80-10 and Mx80-11 have been previously presented in technical reports by Harrington & Horseman (2003) and Harrington & Birchall (2007). However, here we present these results in combination with those from two further tests (Mx80-13 and Mx80-14), providing a larger evidence base from which to compare findings. Our intention is to present laboratory results of the impact of pore-pressure on swelling behaviour in Mx80 bentonite and, in particular, the influence of cyclic applied pressure changes. This is intended as an observational paper, as further expansion of the dataset is required in order to reliably interpret the findings.

## Methodology

### *Experimental set-up*

The experiments described here were carried out using custom-designed constant volume and radial flow (CVRF) apparatuses, constructed initially to examine the sensitivity of gas flow in buffer bentonite to test boundary conditions (Harrington & Horseman 2003). The CVRF systems consist of: (a) a thick-walled stainless steel pressure vessel; (b) a fluid injection system; (c) three independent backpressure systems, each consisting of an array of four filters acting as fluid sinks; (d) five total stress sensors to measure radial and axial stress; and (e) a logging system. The pressure vessel (Fig. 1) comprises a stainless-steel steel, dual-closure, tubular vessel whose end-closures are secured by 12, high-tensile cap-screws that can also apply a small pre-stress to the specimen if required. The positions of the sink arrays ([1], [2] and [3]) and the stress sensors (labelled PT1, 2, 3, 5 and 6) are shown in Figure 1.

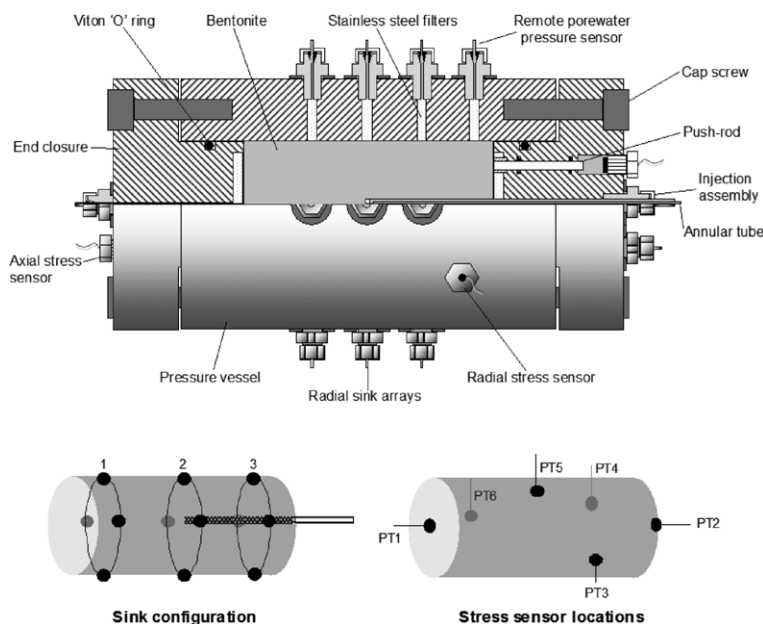


**Fig. 1.** Cut-away section of the constant volume radial flow (CVRF) cell, showing the two end-closures with their embedded drainage filters, the central fluid injection filter, the 12 radial sink filters, the five total stress sensors and the independent pore pressure sensor.

Two CVRF apparatuses were used for the tests described in this paper (Fig. 1), which are both based on a similar design. However, a few notable differences are described below. In CVRF1, all ports, except those for the direct measurement of stress, contain sintered stainless steel porous filters which are profiled to match the bore of the pressure vessel. The stress gauges are an in-house design, using a steel push-rod fitted with an 'O'-ring seal, to compress a small volume of liquid contained within a chamber at the front face of a miniature Sensotec Model pressure transducer. This rig also has a port with an independent pore-water pressure sensor (PT4, Fig. 1), where the push-rod is replaced by a sintered stainless steel porous filter, enabling water pressure to act on the front face of the transducer.

CVRF2 has no pore-pressure sensor directly connected to the pressure vessel itself, but the three pore-pressure arrays can be isolated in connection to a pressure transducer, allowing independent monitoring of the pore-water pressure, or connected to the backpressure pump in order to monitor outflow. While sintered stainless steel filters are embedded in the end closures and the central injection rods of both apparatuses, in CVRF2 the radial arrays contain sintered high-density polyethylene plugs. In this set-up, stress measurements are made using push-rods which are each in direct contact with a Burster miniature load cell (model 8402-6005). In both cases, the central filter is embedded at the end of a 6.4 mm-diameter stainless steel tube which can be used to inject permeant, for gas flow testing purposes. Results from the gas

**Table 1.** Pre-test (calculated with an assumed grain density of  $2.77 \text{ mg m}^{-3}$ )

Sample no.	Moisture content (%)	Bulk density ( $\text{mg m}^{-3}$ )	Dry density ( $\text{mg m}^{-3}$ )	Void ratio	Saturation (%)	Test apparatus
Mx80-10	26.7	2.005	1.582	0.751	98.6	CRVF1
Mx80-11	25.6	2.016	1.605	0.726	97.6	CVRF1
Mx80-13	20.1	2.064	1.718	0.612	91.1	CVRF2
Mx80-14	26.6	1.999	1.579	0.754	97.7	CVRF2

**Table 2.** *Post-test*

Sample no.	Saturation (%)	Maximum $p_w$ experienced (MPa)	Duration of test (days)
Mx80-10	$\geq 100^*$	7	93
Mx80-11	$\geq 100^*$	46	340
Mx80-13	$\geq 100^*$	42	140
Mx80-14	$\geq 100^*$	41	152

\*Measured value indicates sample was fully saturated, within uncertainty limits of the measurement.

testing phase of these experiments are not the focus of this paper and are in preparation for publication or presented elsewhere (Graham *et al.* 2012).

The pressure and flow rate of test fluid is controlled using either an ISCO Teledyne-100 or an ISCO Teledyne-260, Series D syringe pump, operated by an ISCO pump controller. These units have an RS232 serial port, which allows volume, flow rate and pressure data from each pump to be transmitted to a bespoke logging system. Additional test parameters are logged simultaneously by the same system and the typical acquisition

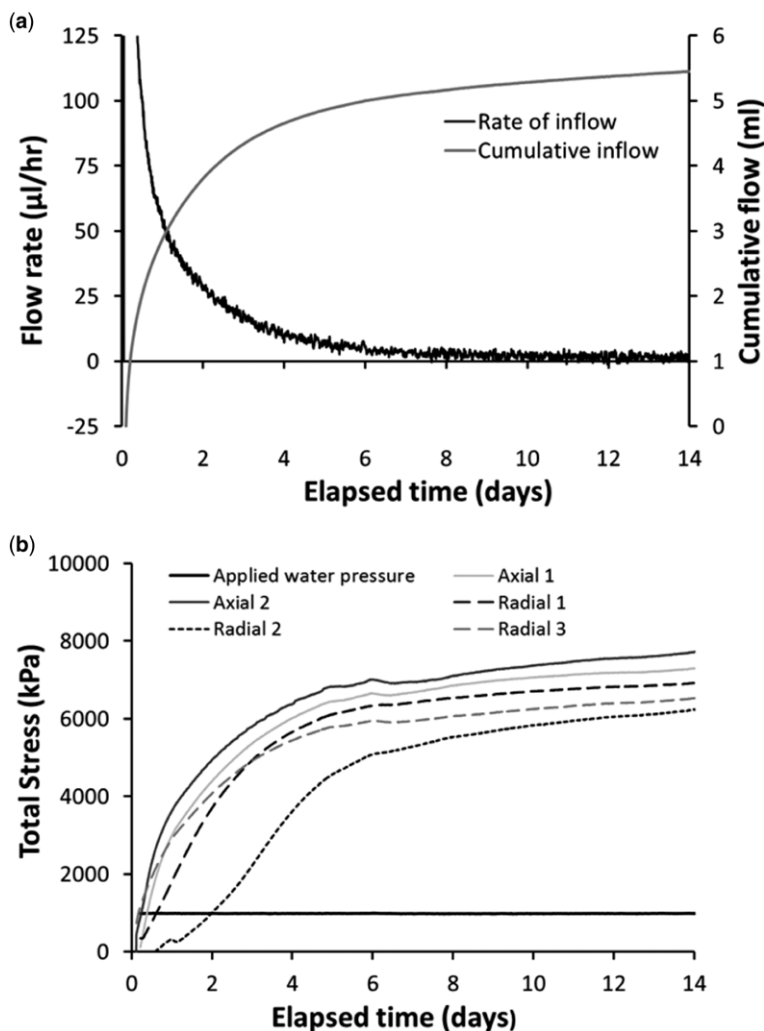


**Fig. 2.** All samples were initially hydrated at a constant applied pore-water pressure of 1 MPa and allowed to re-equilibrate. (a) A typical inflow during the hydration phase test Mx80-14. (b) Both axial and radial stresses were clearly observed to increase during sample swelling (test Mx80-14).

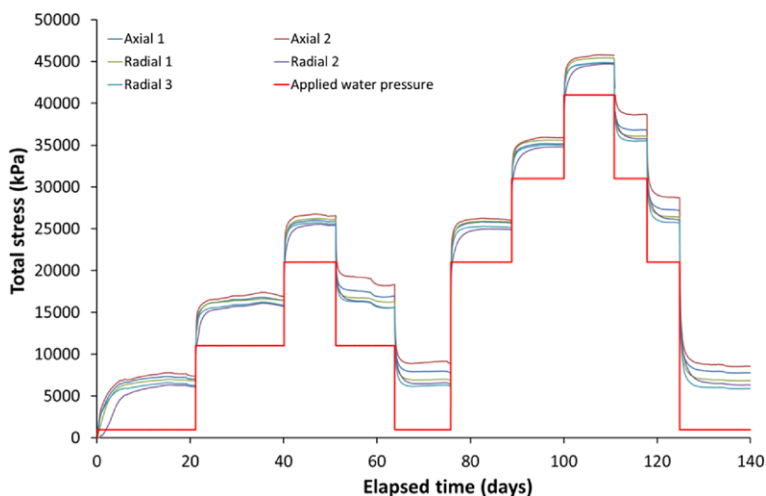


**Fig. 3.** A typical applied water pressure loading history, applied to sample Mx80-14. In the test shown, two loading and unloading cycles were applied to the specimen over the course of 152 days. The stress response observed in this test is atypical, in that no hysteresis was observed (see Fig. 6a).

rate is one scan every 2 min. All stress and pore pressure sensors were calibrated against laboratory standards by applying incremental steps in pressure, from atmospheric pressure to a pre-determined maximum value. This was followed by a descending history to quantify any hysteresis.

### Sample preparation and properties

Testing was carried out on samples of Mx80 bentonite, which is the selected buffer material for the Swedish radioactive waste repository concept. Mx80 bentonite is a fine-grained sodium bentonite, from Wyoming, which contains around 80% montmorillonite (Karlund 2010). Blocks of pre-compacted bentonite were manufactured by Clay Technology AB (Lund, Sweden), by rapidly compacting bentonite granules in a mould under a one dimensionally applied stress (Johannesson *et al.* 1995). In this paper, results are presented from experiments carried out on four cylindrical test specimens (with a diameter = 60 mm and length = 120 mm), sub-sampled from the bentonite. Samples Mx80-10 and Mx80-11 were manufactured by hand-trimming using a tubular former with a sharpened leading edge. The upper and lower surfaces were finished using a scraping action with a flat-bladed knife, leaving the end surfaces flat and parallel. The former was mounted in a lathe and a 6.4 mm-diameter hole drilled in the clay to accommodate the source filter and tubing assembly. The specimen was then extruded from the former into the pressure vessel using a screw-driven press.

Rather than using the former, samples Mx80-13 and Mx80-14 were instead turned to the same dimensions on a lathe, producing a high quality finish on the cylindrical surface, and a hole drilled into the clay as before.

Standard geotechnical properties for each sample pre- and post-test are shown in Tables 1 and 2, respectively. The water content of the specimens was determined by weighing them pre-test, then oven-drying them post-test before weighing again. The void ratio, porosity and degree of saturation are based on a grain density for the bentonite of  $2.77 \text{ mg m}^{-3}$  (taken from an average of the values measured by Karlund 2010). Dry densities of the samples were *c.*  $1.55\text{--}1.75 \text{ mg m}^{-3}$  and, therefore, above the dry density of  $1.4 \text{ mg m}^{-3}$  where Bucher & Müller-Vonmoos (1989) noted a change in the relationship between applied water pressure and the resulting stress generated.

### Pore-pressure cycling

For each sample, hydration was carried out with de-ionized water, applied through all filters. A high-precision syringe pump was used to maintain a constant applied water pressure, while the rate of inflow, and consequent stress development, were monitored. Each test was begun by applying a constant applied water pressure of 1 MPa. An example showing the typical stress development and rate of inflow (for sample Mx80-14) is given in Figure 2. The monitored stresses are shown as measured in three radial locations, as well as

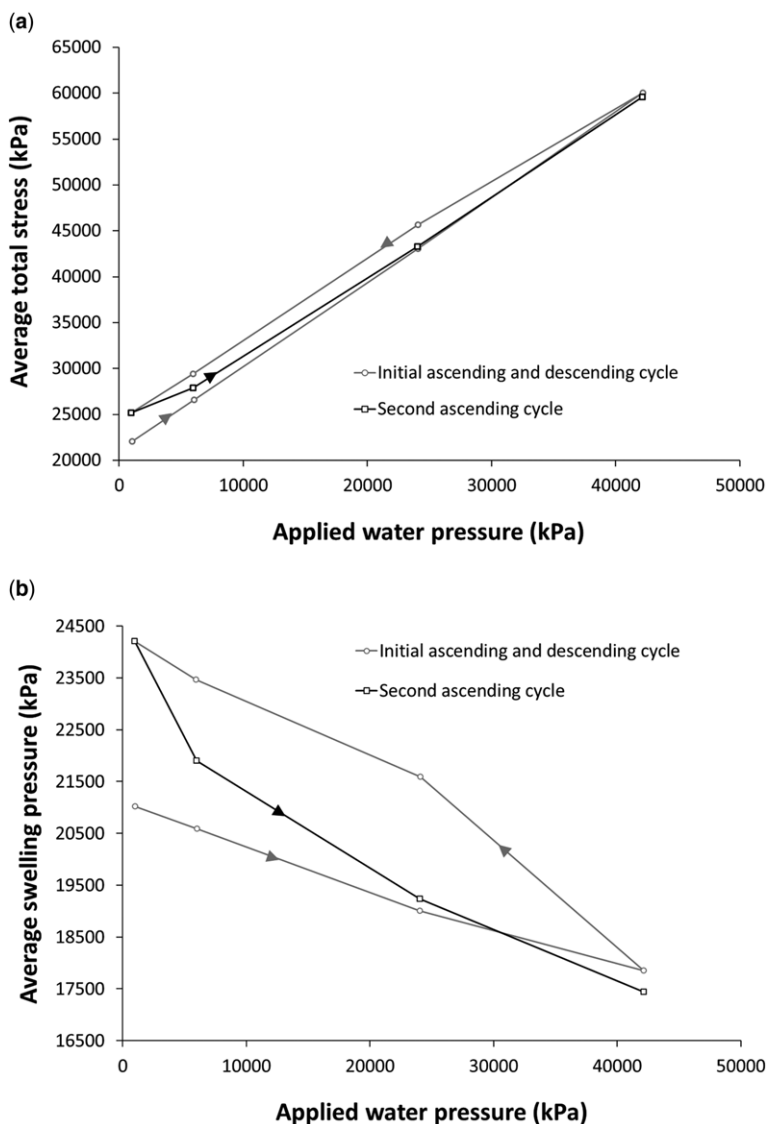


**Fig. 4.** (a) An example stress response history, resulting from applied water pressure cycling (for sample Mx80-13). (b) An example swelling pressure response history, resulting from applied water pressure cycling (for sample Mx80-13).

at the samples ends (axial). The drop-off in water inflow, as the rate of sample swelling slowly reduces and the clay equilibrates with the applied water pressure, is clearly shown. For all water pressure increments, the sample was only subjected to a new applied pressure once this stage had been clearly reached.

Each sample was subjected to a series of incremental constant pore pressure steps, with all samples experiencing at least one loading and unloading cycle. Samples Mx80-10 and Mx80-14

were subjected to one and two full cycles, respectively. In the case of specimen Mx80-11, three cycles were carried out (the last two with smaller pressure steps) and specimen Mx80-13 was subject to one full cycle, plus additional loading increments. In an ideal system (where alpha equals one), swelling pressure,  $\Pi$ , is equal to the effective stress (Harrington & Birchall 2007). In order to examine the validity of this relationship, swelling pressure was calculated using this assumption, as shown in the following section.

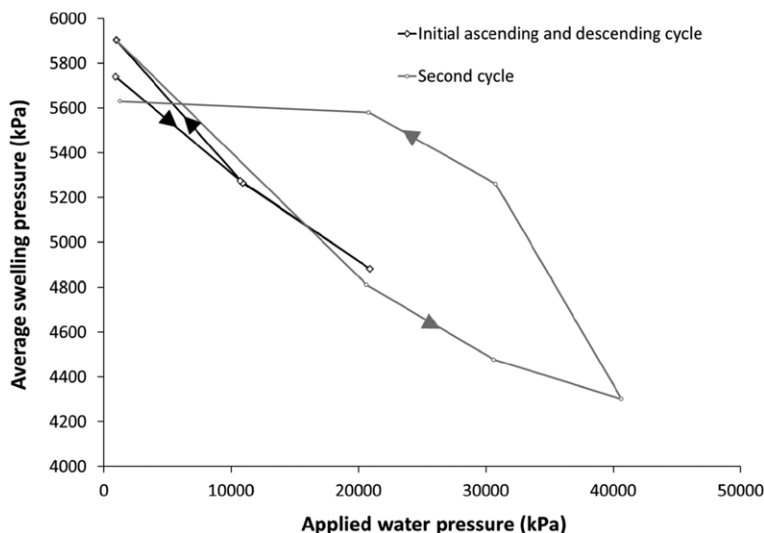


Fig. 5. An example swelling pressure response history, resulting from applied water pressure cycling (for sample Mx80-14).

## Results

In this section we present results from all four experiments. A typical loading history is shown in Figure 3 (for sample Mx80-14), which demonstrates the significant timescales required to carry out testing of this nature. The measured dry and bulk densities for each sample are given in Table 1. All samples were found to be fully saturated after testing was completed (Table 2). An example loading history is shown in Figure 4 (for Mx80-14), along with generated total stresses (at three radial and two axial locations) and calculated swelling response. For all tests, the swelling pressure was clearly observed to decrease with increasing pore-water pressure (e.g. Fig. 5 – Mx80-14). This behaviour was observed by Harrington & Horseman (2003) at lower water pressures. However, by investigating the form of this relationship over a more extensive range of pressures, it is clear that the sensitivity of the swelling pressure to changes in the applied water pressure decreases asymptotically as  $p_w$  is increased (Fig. 5). This implies that, within the range of expected repository conditions, there is a physical limit beyond which swelling pressure becomes insensitive to further increases in applied water pressure, most likely owing to the reduced mobility of water within the clay under these conditions. As such, care must clearly be taken when attempting to extrapolate swelling pressure behaviour at higher pore-water pressures, based on laboratory data measured at lower applied pressures.

In addition, the results from cycling loading and unloading of the bentonite indicate that pore-pressure cycling may lead to a persistent elevation in the average swelling pressure of the clay, in spite of a consequent reduction in the applied pore-water pressure. By plotting the measured average total stress and the calculated swelling pressure at each applied pressure step (Fig. 6), a significant degree of hysteresis is made apparent for samples Mx80-10, Mx80-11 and Mx80-13. Higher density bentonite was used for test Mx80-13, explaining the noticeably higher total stresses and swelling pressures observed. However, hysteresis was still clearly observed at these higher pressures. In the case of sample Mx80-14, the observed behaviour is anomalous: while significant non-linearity in the behaviour of the bentonite (Fig. 5) was apparent, the resulting swelling pressure after the first and second pore-pressure cycles did not significantly deviate from the initially measured values. Incremental values for  $\alpha$  were calculated, by fitting to the slope of the measured stress v. the applied water pressure between each step (i.e. calculating  $d\sigma/dp_w$ ). The average total stress data for all tests yield incremental  $\alpha$  values generally within the range 0.8–1.0 (Fig. 7), which is in agreement with previous results for Mx80 bentonite (Bucher & Müller-Vonmoos (1989)). It should be noted that the initial elevated swelling pressures observed in sample Mx80-13 were the result of a significantly higher starting dry density of the material (Table 1).

However, the observed differences in behaviour for Mx80-14 do not appear to be explained

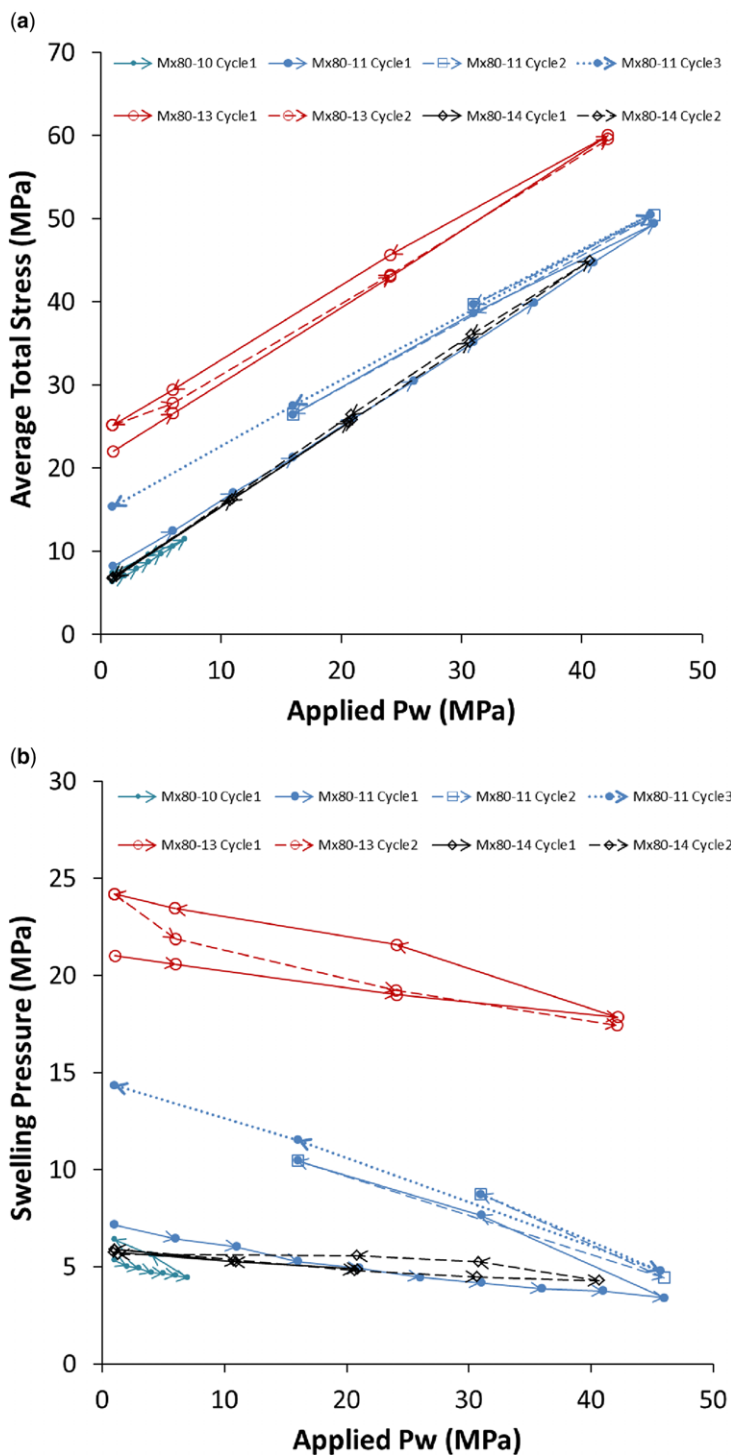


**Fig. 6.** (a) Average total stress plotted against externally applied water pressure (backpressure). (b) Swelling pressure plotted against externally applied water pressure (backpressure). Samples Mx80-11 and Mx80-13 show a clear departure from the predicted ideal behaviour, as does Mx80-10 (as a percentage of the initial swelling pressure).

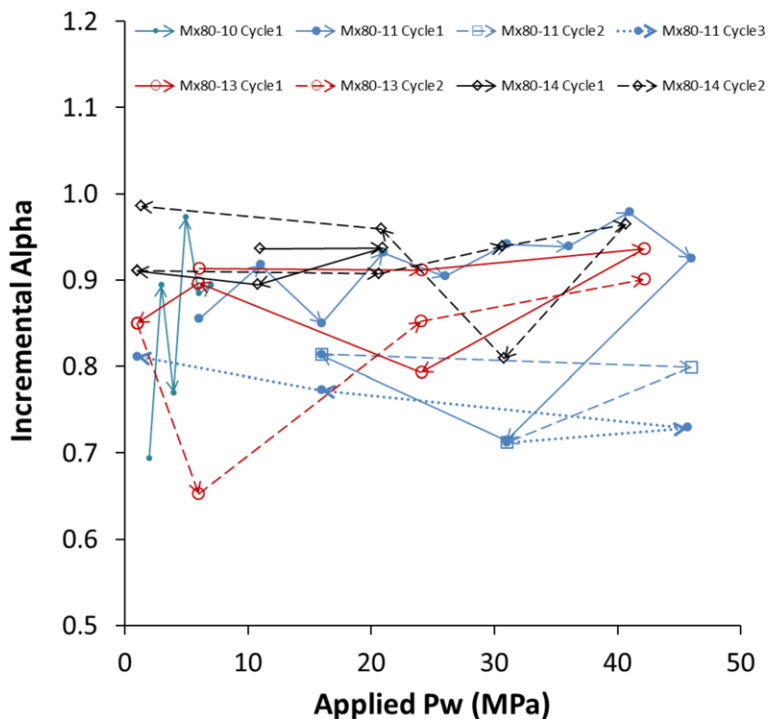


**Fig. 7.** Calculated incremental values of  $\alpha$  (a proportionality constant equal to  $d\sigma/dp_w$ ), resulting from applied water pressure cycling (for all four samples of Mx80 bentonite).

simply by dry density alone. While a different stress measurement method was utilized in test Mx80-14, hysteric behaviour was observed for sample Mx80-13, which was conducted with the same experimental apparatus. Care was taken to ensure that samples were at hydraulic equilibrium before calculating the resulting swelling pressure. Time may be another potential influence on the observed behaviour though, if a degree of time-dependency exists in the response of the bentonite. However, no evidence for such time dependency could be observed when comparing the length of pressure steps for experiments within this dataset. Instead, it seems more likely that the observed hysteresis is an artefact of the underlying physics governing bonding of water to the clay and its coupling to the stress state of the sample. However, further expansion of the data set is required in order to better elucidate the cause of and controls on this observed behaviour.

## Conclusions

In order to examine the form of the relationship between swelling pressure and applied water pressure, a series of pressure cycling experiments were

conducted on samples of pre-compacted Mx80 bentonite. The experiments were conducted using a specially designed constant volume cell, which allows the evolution of the total stresses acting on the surrounding vessel to be monitored during clay swelling. The results clearly demonstrate a significant decrease in swelling pressure with increase applied water pressure, for all four Mx80 samples. However, it is also apparent that this sensitivity to changes in applied water pressure is significantly reduced at more elevated values of  $p_w$ .

In addition to this observed non-linearity in behaviour, test observations also indicate that an elevated swelling pressure may be retained at significant magnitudes within the clay, as a result of a cyclic water pressure loading. While the observed behaviour is not extreme in magnitude, the effect is notable and suggests that our understanding of the relationship between applied water pressure and swelling pressure is not yet complete. As such, a better understanding of the causes of this behaviour may be needed when assessing repository performance in response to periods of elevated or decaying pore-water pressure (e.g. during interglacial and glacial events). However, it should also be noted that such hysteric behaviour is not always observed and the cause of this remains, as yet,

unclear. Further testing will help to clarify the controls on this behaviour and to elucidate the nature of the relationship between pore-water pressure, swelling pressure and the resulting total stress in such systems.

The research leading to these results has received funding from SKB and the European Atomic Energy Community's Seventh Framework Programme (FP7/2007-2011) under Grant Agreement no. 230357, the FORGE project. We would like to thank the reviewers for their comments and improvements. This paper is published with the permission of the Executive Director of the British Geological Survey (NERC).

## References

- BASMA, A. A., AL-HOMOUD, A. S., HUSEIN MALKAWI, A. I. & AL-BASHABSHEH, M. A. 1996. Swelling-shrinkage behaviour of natural expansive clays. *Applied Clay Science*, **11**, 211–227.
- BÖRGESSON, L. 1985. Water flow and swelling pressure in non-saturated bentonite-based clay barriers. *Engineering Geology*, **21**, 229–237.
- BUCHER, F. & MÜLLER-VONMOOS, M. 1989. Bentonite as a containment barrier for the disposal of highly radioactive wastes. *Applied Clay Science*, **4**, 157–177.
- DOOSTMOHAMMADI, R., MOOSAVI, M. & ARAABI, B. N. 2008. A model for determining the cyclic swell-shrink behaviour of argillaceous rock. *Applied Clay Science*, **42**, 81–89.
- GRAHAM, C. C., HARRINGTON, J. F., CUSS, R. J. & SELLIN, P. 2012. Gas migration experiments in bentonite: implications for numerical modelling. *Mineralogical Magazine*, **76**, 3279–3292.
- HARRINGTON, J. F. & BIRCHALL, J. D. 2007. *Sensitivity of total stress to changes in externally applied water pressure in KBS-3 buffer bentonite*. SKB Silver Series Technical Report **TR-06-38**, Svensk Kärnbränslehantering AB, Stockholm.
- HARRINGTON, J. F. & HORSEMAN, S. T. 2003. *Gas migration in KBS-3 buffer bentonite: sensitivity of test parameters to experimental boundary conditions*. Report **TR-03-02**, Svensk Kärnbränslehantering AB, Stockholm.
- JOHANNESON, L.-E., BÖRGESSON, L. & SANDÉN, T. 1995. *Compaction of bentonite blocks: development of technique for industrial production of blocks which are manageable by man*. TR 95-19, Svensk Kärnbränslehantering AB.
- KARNLAND, O. 2010. *Chemical and mineralogical characterization of the bentonite buffer for the acceptance control procedure in a KBS-3 repository*. Report **TR-10-60**. Svensk Kärnbränslehantering AB (SKB), Stockholm.
- MADSEN, F. T. & MÜLLER-VONMOOS, M. 1989. The swelling behaviour of clays. *Applied Clay Science*, **4**, 143–156.
- OSCARSON, D. W., DIXON, D. A. & GRAY, M. N. 1990. Swelling capacity and permeability of an unprocessed and a processed bentonitic clay. *Engineering Geology*, **28**, 281–289.
- OSIPOV, V. I., BIK, N. N. & RUMJANTSEVA, N. A. 1987. Cyclic swelling of clays. *Applied Clay Science*, **2**, 363–374.
- PEJON, O. J. & ZUQUETTE, L. V. 2002. Analysis of cyclic swelling of mudrocks. *Engineering Geology*, **67**, 97–108.
- PUSCH, R. 1980. *Swelling pressure of highly compacted bentonite*. Report **TR-80-13**. Svensk Kärnbränslehantering AB, Stockholm.
- SVENSK KÄRNBRÄNSLEHANTERING AB 2011. *Long-term safety for the final repository for spent nuclear fuel at Forsmark: main report of the SR-site project*. TR-11-01.
- TERZAGHI, K. 1943. *Theoretical Soil Mechanics in Engineering Practice*. John Wiley, New York.